Available online at www.sciencedirect.com
SCIENCE DIRECT®

Polymer 44 (2003) 4863–4870

polymer

www.elsevier.com/locate/polymer

Poly(vinyl pyrrolidone)—C_{70} complexes in aqueous solutions

Elvira Tarassova[a], Vladimir Aseyev[a,b,*], Heikki Tenhu[b], Stanislav Klenin[a]

[a]*Institute of Macromolecular Compounds, Russian Academy of Science, Bolshoi Prospect 31, 199004 St. Petersburg, Russian Federation*
[b]*Laboratory of Polymer Chemistry, PB 55, FIN-00014 HY, University of Helsinki, Helsinki, Finland*

Received 10 December 2002; received in revised form 12 May 2003; accepted 30 May 2003

Abstract

Aqueous solutions of poly(vinyl pyrrolidone)–fullerene complexes (PVP–C_{70}) have been studied using static and dynamic light scattering methods. Two diffusive processes were detected. The slow diffusion was interpreted as dynamics of large intermolecular PVP–C_{70} complexes while the fast diffusion was associated with the presence of individual PVP molecules in solution. It was also shown that the molecular weights and dimensions of PVP–C_{70} complexes are smaller than for PVP–C_{60} by a factor of 2.5–3. In aqueous solutions of PVP–C_{70} complex the depolarization and dissymmetry of scattered light were observed in contrast to PVP–C_{60} solutions. It reveals the existence of anisotropic structures in PVP–C_{70} solutions. Intermolecular interactions within PVP–C_{70} complexes are weak and a hydrodynamic field can destroy complexes.

© 2003 Published by Elsevier Science Ltd.

Keywords: Fullerene–polymer complex; Static and dynamic light scattering; Aqueous solutions

---

1. Introduction

Scientific interest to fullerenes rises with respect to their biological activity [1–5]. For example, a large number of fullerene and fullerene derivatives are competitive inhibitors of the human immunodeficiency virus protease thanks to its specific shape, which fits into the hydrophobic cavity of the enzyme active site [1]. It can also be mentioned that fullerenes are able to generate efficiently cytotoxic singlet oxygen ($^1O_2$) making them promising compounds for antitumour activities (photodynamic therapy; DNA can be cleaved by reaction with $^1O_2$ generated by C_{60}) [2–4]. However, the investigation of biological effects of fullerenes has been hindered by their insolubility in water. One of the ways to resolve this problem is to form fullerene containing complexes of hydrophilic polymers such as poly(vinyl)pyrrolidone (PVP). This way seems to be more favorable than if a hydrophilic polymer is covalently bound to a fullerene molecule. In the fullerene containing complexes, the initial structure of fullerene is almost intact. On the other hand, the biological activity of polymer–fullerene complexes may not be related to their chemical composition only. It is also essential to determine the structure and conformation of fullerene containing polymer complexes in aqueous solutions.

Polymer–fullerene complexes and polymeric composites with fullerenes are of a special interest owing to a non-destructive nature of polymer interaction with the unique electron structure of fullerenes. Fullerenes are known to have a partial surface charge owing to their free π-electrons. As has been revealed recently, the complexes of poly(vinylpyrrolidone) with fullerene C_{60} are formed due to the formation of donor–acceptor bonds between fullerene and the carbonyl groups of the polymer [5–7].

Properties of aqueous solutions of PVP–C_{60} complexes have been investigated by various methods (NMR, UV-spectra, SLS, DLS, diffusion, viscosity) [6–13]. The fullerene C_{60} was found to aggregate in aqueous media [8]. But in PVP–fullerene complexes, the mentioned tendency of hydrophobic fullerenes competes with hydrophilic repulsion between polymer molecules, and the strong intermolecular interactions have been detected in light scattering experiments [9–13]. Two diffusion modes were detected in aqueous solutions of PVP–C_{60} complexes by dynamic light scattering (DLS). The fast mode was suggested to represent the translation diffusion of individual

---

* Corresponding author. Address: Institute of Macromolecular Compounds, Russian Academy of Science, Bolshoi Prospect 31, 199004 St. Petersburg Russia..

E-mail address: vladimir.aseyev@helsinki.fi (V. Aseyev).

0032-3861/03/$ - see front matter © 2003 Published by Elsevier Science Ltd.
doi:10.1016/S0032-3861(03)00477-4

complexes. The origin of the slow mode was explained in terms of strong interaction between complexes. Naturally, it is interesting to find out what happens when C_{60} is replaced with C_{70}. As it is known, the geometrical shape of fullerene molecules defines the character of π-electron density distribution over the molecule surface [14]. Indeed, as it was established by the quantum analysis for a spherical C_{60} fullerene π-electronic density is uniformly distributed on an inner surface of a molecule. For a fullerene with a prolate shape (such as C_{70}) some of the electronic density sites shift towards the outer surface of a fullerene molecule. Therefore, polymer–fullerene C_{70} complexes may have physical and chemical properties different from polymer–C_{60} complexes. Besides, the structure and dynamics of PVP–fullerene complexes based on C_{70} practically have not been investigated. To our knowledge, this is at least one of the first experimental attempts to study the aqueous solutions of PVP–C_{70} systems.

2. Experimental part

2.1. Materials

The PVP–C_{70} complexes were prepared at the Institute of Experimental Medicine RAMS (St. Petersburg, Russia) from PVP of $M_w = 10 \times 10^3$, 25×10^3, 40×10^3, 46×10^3 g/mol (Merck) and fullerene C_{70} of 99% of purity (Fullerene Technologies, Russia) using the method described in Ref. [15]. However, herein benzene was used as a solvent for C_{70} instead of toluene. This allowed the complex to be purified of solvent under mild conditions. All polymer samples were characterized by static light scattering (SLS) in aqueous solutions, M_w/M_n was found to be 1.1–1.3 for all the samples. The PVP–C_{70} systems were prepared with various relative contents of fullerene C_{70} (0.21–0.63 wt% with respect to the weight of pure PVP). Fullerene content in the complexes was determined from the UV absorption spectra of the aqueous solutions of the samples.

Aqueous solutions were prepared from dry PVP–C_{70} samples in de-ionized bi-distilled water. Water was de-ionized with an ELGASTAT UHQ-PS device. The solutions were investigated in the range of complex concentration from 0.2 to 2.5 mg/ml. All polymer solutions and solutions of PVP–C_{70} complexes were purified of dust using filter units of 0.45 μm pore size (Millex, PVDF filter).

Table 1 represents the compositions and molecular parameters of the investigated samples (molar masses of parent PVP samples and fullerene contents in the complexes).

2.2. Instrumentation

All samples were investigated using methods of light scattering. SLS was measured at 90° scattering angle with a Sofica device (model 42.000 Photo-Gonio-Diffusometer, the instrument used with a Wratten-61 filter adapted to the $\lambda = 546$ nm wavelength of the SP500 mercury lamp). The device was calibrated using benzene as a calibrating standard. DLS as well as SLS experiments were also performed using a Brookhaven Instrument BIC-200 SM goniometer and BIC-9000 AT digital correlator. An argon laser (LEXEL 85, 1W) having $\lambda = 514.5$ nm wavelength was the light source. Correlation functions were collected with the shortest sample time 0.1–2.0 μs, whereas the last delay was 8–10 ms. Data has been analyzed with Brookhaven Instruments software (CONTIN: 6KDLSW, Beta version 1.30). The BIC device was calibrated using toluene as a calibrating liquid. Scattered light was collected between 30 and 150° scattering angles in both SLS and DLS experiments. 5 to 7 correlation curves with various accumulation times were collected for every sample to check the reliability of the mathematical solution by CONTIN program. Increment of refractive index dn/dc was measured using a refractometer (IRF 23, Russia). dn/dc values for solutions of PVP–C_{70} complexes with varying fullerene content were $dn/dc = 0.171 \pm 0.002$ ml/g. For pure PVP dn/dc was 0.167 ± 0.002 ml/g. The experiments were performed at 20 ± 0.1 °C.

3. Methods

In SLS experiments, the time-averaged intensity of scattered light was collected as a function of sample concentration c and scattering angle θ. When extrapolated to zero scattering angle and zero concentration, such measurements yield the weight-averaged molar mass M_w, the radius of gyration R_g and the second osmotic virial coefficient A_2 of the scattering objects [16]. Thus, in cases when scatterers are large, the excess scattered intensity is dependent of scattering angle, and the Zimm equation applies

$$\frac{Kc}{R_\theta} = \frac{1}{P(\theta)M_w} + 2A_2c \tag{1}$$

where K is the optical constant given by

$$K = \frac{4\pi^2 n_0^2 (dn/dc)^2}{N_A \lambda_0^4} \tag{2}$$

The radius of gyration can be obtain from Zimm plot by

$$(\bar{R}_g^2)^{1/2} = \frac{\sqrt{3}\lambda_0}{4\pi n_0}(s_0 M_w)^{1/2} \tag{3}$$

In the Eqs. (1)–(3), R_θ is the excess intensity of light scattered at the angle θ represented as the Rayleigh ratio; cK/R_θ is the reciprocal of reduced scattering intensity; $P(\theta)$ is the particle scattering factor representing angular dependence of scattered light; N_A is the Avogadro number; λ_0 is the wavelength of the incident laser light source; n_0 is the refractive index of the solvent; dn/dc is the refractive

Table 1
Static and dynamic light scattering results for aqueous solutions of PVP–C_{70} complex obtained at 90° scattering angle

Sample no.	Complex component		Complex parameters						
	M_{PVP} (g/mol)	C_{ful} (wt%)	$M_{\mathrm{w}}^{\mathrm{app}} \times 10^{-6}$ (g/mol)	R_{g} (nm)	$R_{\mathrm{h,f}}^{\mathrm{app}}$ (nm)	$D_{\mathrm{f}}^{\mathrm{ap}} \times 10^{8}$ ($\mathrm{cm^2 s^{-1}}$)	$R_{\mathrm{h,s}}^{\mathrm{app}}$ (nm)	$D_{\mathrm{s}}^{\mathrm{app}} \times 10^{8}$ ($\mathrm{cm^2 s^{-1}}$)
1	10000	0.63	1.7	–	3.5	65	79.0	2.22
2		0.43	0.29	–	–	–	–	–
3		0.21	0.2	–	3.3	67	55.0	3.4
4	24500	0.62	3.3	–	–	–	–	–
5		0.40	0.3	–	–	–	–	–
6	40000	0.63	8.0	–	7.5	29	105.5	2.05
			8.6[a]	123.0[a]	–	–	–	–
7		0.40	0.5	–	7.5	29	88	2.44
			1.2[a]	93.0[a]	7.5[a]	29[a]	115[a]	2.0[a]
8	46300	0.55	8.5	–	–	–	105	2.05
			17.2[a]	214.0[a]			125[a]	1.8[a]
9		0.28	1.0	–	–	–	–	–

[a] Obtained for zero scattering angle.

index increment of the scattering species; s_0 is the initial slope of the $(cK/R_\theta)_{c=0} = f(\sin^2(\theta/2))$.

In DLS experiments, the autocorrelation function of scattered light intensity $G_2(t) = \langle I(0)I(t)\rangle$ was collected and then converted into an autocorrelation function of the scattered electric field $g_1(t)$ using the Siegert's relationship [17]

$$|g_1(t)| = \beta^{1/2}\sqrt{\frac{G_2(t) - G_2(\infty)}{G_2(\infty)}}, \tag{4}$$

where $G_2(\infty)$ is the experimentally determined baseline, and β is the coherence factor determined by the geometry of the detection (typically $0.5 \le \beta \le 0.8$). Characteristic decay times of a field correlation function τ_{i} and their relative amplitudes $A_{\mathrm{i}}(\tau_{\mathrm{i}})$ were evaluated via moments of a corresponding distribution function of decay times $A(\tau)$ obtained using the inverse Laplase transform program CONTIN as

$$g_1(t) = \int_0^\infty A(\tau)\mathrm{e}^{-t/\tau}\,\mathrm{d}\tau, \tag{5}$$

Translation diffusion coefficients were calculated as $D_{\mathrm{i}} = (1/\tau_{\mathrm{i}})q^{-2}$, where q is the scattering vector determined as $q = (4\pi n_0/\lambda_0)\sin(\theta/2)$. The hydrodynamic radii were obtained from the diffusion coefficient D_{i} via the Stokes–Einstein equation

$$R_{\mathrm{hi}} = \frac{kT}{6\pi\eta_0 D_{\mathrm{i}}}, \tag{6}$$

where k is the Boltzmann constant, T is the absolute temperature, and η_0 is the solvent viscosity. Mean average values of the hydrodynamic radius distributions were used for the estimation of the average radii R_{h}.

4. Results and discussion

4.1. Static light scattering

First of all, to make sure that the investigated samples in aqueous solutions do not absorb light, absorption measurements were performed in the wavelength range, where the light scattering is measured. The absorption spectrum of the sample 6 with concentration $c = 2.8$ mg/ml and of the sample 8 with $c = 2.0$ mg/ml were measured in the region of wavelengths $\lambda = 400 - 800$ nm (note that the wavelength of the light sources used in the scattering experiments was 546 and 514 nm). It was found that light absorption of the solutions at 546 and 514 nm is negligibly small and thus, the measured light scattering from these samples is not affected by absorption.

Aqueous solutions of fullerene free PVP and fullerene C_{70} containing samples were studied using SLS. Fig. 1 represents selected results of these investigations obtained at 90° scattering angle. Curve 1 in the inset of Fig. 1 shows the plot of $cK/R_{90°}$ vs. PVP concentration. It can be seen that

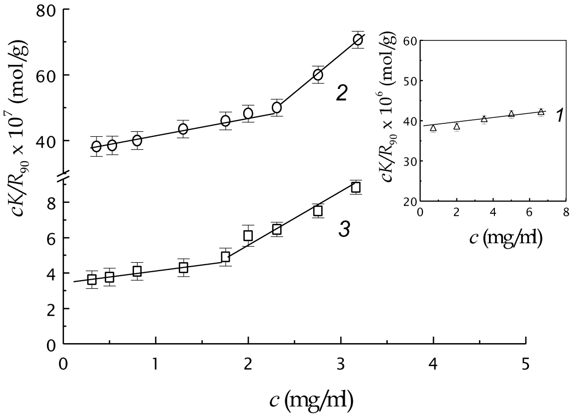

Fig. 1. cK/R_{90} vs. concentration c for aqueous solutions of PVP (1; inset) and PVP/C_{70} complex with equal molar masses of the matrix PVP: sample 5 (2) and sample 4 (3).

the $cK/R_{90°}$ ratio increases linearly with PVP concentration. No angular dependence of the scattered light intensity was observed. The extrapolated value of the molar mass $M_w = 26 \times 10^3$ g/mol is in a good agreement with the value given by the manufacturer, i.e. $M = 25 \times 10^3$ g/mol.

On the other hand, SLS experiments on aqueous solutions of PVP–C_{70} demonstrated that the scattered intensity does not exhibit any classical c and q (angular) dependences. The concentration dependence of the reciprocal reduced intensity of scattered light for solutions of PVP–C_{70} has two linear regions (as for PVP–C_{60} as well [9–13]); see curves 2 and 3 representing samples 4 and 5, respectively. In the more concentrated solutions, i.e. above a critical concentration, c_{cr}, where the slope changes, the scattering intensity is independent of concentration (i.e. R_θ is constant). This means that $(cK/R_\theta) = \text{const}\ c$ and M_w is infinitely large if extrapolated to zero concentration from this concentration region. Below the critical concentration c_{cr}, the extrapolation to zero concentration gives finite values of molar mass M_w^{app}. The values are apparent ones, since recorded at 90° scattering angle. Values of M_w^{app} obtained from the lower concentration region for all samples studied, are higher than that for the matrix polymer PVP by 1–2 orders of magnitude. Taking into account the existing angular dependence of the scattered light intensity, one may expect even higher values of the actual molar masses measured at zero scattering angles, see Table 1. This indicates that in these solutions the polymer molecules form large intermolecular complexes with fullerene (below, these will be called IMC PVP–C_{70}).

As can be seen from Table 1, the molecular weight of PVP–C_{70} exhibits a pronounced increase with an increasing fullerene content while M_{PVP} is kept constant (and it is similar to PVP–C_{60} complex). These facts are somewhat expected if PVP–C_{70} complexes form in water. Thus, the increasing fullerene content may lead to increasing number of C_{70} hydrophobically attached to PVP molecules and to increasing number of intermolecular crosslinks via C_{70} molecules. An increase in M_{PVP} leads to an increase in the apparent molecular weight of PVP–C_{70} while fullerene content is kept constant. Numerous SLS experiments on PVP–C_{70} demonstrated the stability of the samples with time. The position of c_{cr} and the apparent molecular weights of PVP–C_{70} samples do not depend on the history of solution preparation.

The existence of the critical concentration c_{cr} is interesting. It should be noted that in all investigated solutions of PVP–C_{70} with the same C_{70} content, the critical concentration is almost constant (2.0 mg/ml). However, if the M_{PVP} is kept constant, c_{cr} decreases with increasing fullerene content. For instance, c_{cr} was found to be 2.3 mg/ml for a sample with 0.2 wt% of fullerene while for 0.6 wt%, c_{cr} was 1.8 mg/ml. The origin of c_{cr} is not clear. It may be associated with the transition from a dilute into a semidilute solution of the PVP–C_{70} complex. In this case the PVP–C_{70} complexes overlap above c_{cr} forming a network, and the light scattering intensity is independent of PVP–C_{70} concentration. The low value of the overlap concentration c_{cr} together with the high M_w values suggests a loose internal structure of the IMC PVP–C_{70} complexes. Increase in M_w of PVP–C_{70} with fullerene content (see Table 1) results in an increasing hydrodynamic size of the IMC PVP–C_{70} and therefore in a decreasing overlap concentration c_{cr}. Increase in M_w of PVP–C_{70} with M_{PVP} is insignificant and the overlap concentration is not much affected. As will be shown later in the text, two types of particles are always present in PVP–C_{70} solutions and the precise calculation of the overlap concentration is not a straightforward procedure.

In the lower concentration region when $c < c_{cr}$, R_θ increases with concentration and interaction between scatterers is minor. Molecular weights of the complexes may in principle be obtained at a zero scattering angle and zero concentration. However, two types of particles have always been observed in all PVP–C_{70} solutions studied. Fig. 2 represents an example of the angular dependence (the q-dependence) of the absolute scattered light intensity R_θ for two solutions of sample 7 with different concentrations. Two linear regions of R_θ vs. scattering angle indicate the coexistence of scatterers with two different sizes. Similar angular dependences were observed for the other samples as well. It has been shown recently using luminescence measurements, that two types of PVP are present in the PVP–C_{60} complexes: PVP bound to individual fullerene molecules and PVP, which is bound to fullerene clusters [18]. This accords with our conclusions.

The dimensions of the complexes and their relative contributions into the total intensity of scattered light remain almost invariable with increasing or decreasing the solution concentration. This conclusion was supported by dissymmetry measurements. Dissymmetry of the scattered light is defined as $z_\theta = R_\theta/R_{180°-\theta}$ and it is related to the size and shape of the particles. It was observed that z_θ does not change upon dilution, see inset in Fig. 2.

Studies on the depolarization of the scattered light

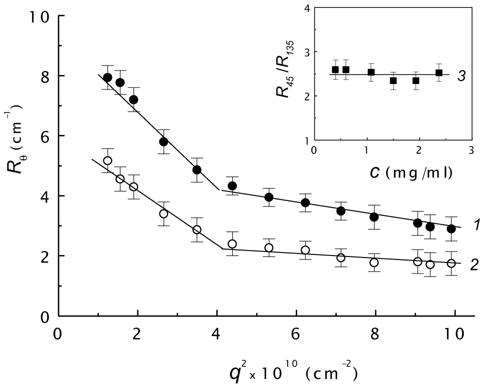

Fig. 2. Angular dependence of the absolute intensity of light scattered by aqueous solutions of PVP/C_{70} (sample 7) with concentrations 2.4 mg/ml (1) and 1.1 mg/ml (2). Inset shows the dissymmetry of scattered light intensity vs. concentration for sample 7 (3).

revealed the anisotropic character of PVP–C_{70} solutions. This was also confirmed using a method of flow birefringence (for the description of this method see Ref. [16]). A solution of sample 8 having the concentration 2.0 mg/ml was investigated. It was found that with increasing shear rate, the solution anisotropy first sharply increases and then suddenly disappears at higher shear rate, while the solution of pure PVP of the same concentration does not show any birefringence. The disappearance of anisotropy may be a result of disintegration of the complex under the applied hydrodynamic field. If the influence of the hydrodynamic field stops, large intermolecular PVP–C_{70} complexes are formed again.

4.2. Dynamic light scattering

Five PVP–C_{70} samples were investigated using DLS (samples 1, 3, 6, 7, and 8). For all PVP–C_{70} solutions studied (excluding sample 8), correlation functions were double exponential and thus, two diffusive processes were observed. These processes were characterized by two diffusion coefficients denoted as fast (D_f) and slow (D_s) modes, respectively. These modes were well separated and obvious at scattering angles between 30 and 150°. The difference between the calculated and measured baselines of the correlation functions collected was less than 0.5%. The average error of CONTIN residuals was less than 5×10^{-3}. For each of the PVP–C_{70} solutions, 5–7 correlation functions at a fixed angle were collected and the average values of the diffusion coefficients were taken for further analysis.

Fig. 3 shows an example of a normalized correlation function of scattered light intensity $g_2(t)$ collected for sample 3 at 90° scattering angle and 1.4 mg/ml concentration. Corresponding correlation function of the electric field $g_1(t)$ is presented in the inset of the Fig. 3 in lognormal scale. Solid line shows a fit by CONTIN. Corresponding distribution of hydrodynamic radius is obviously bimodal and presented in Fig. 8(b).

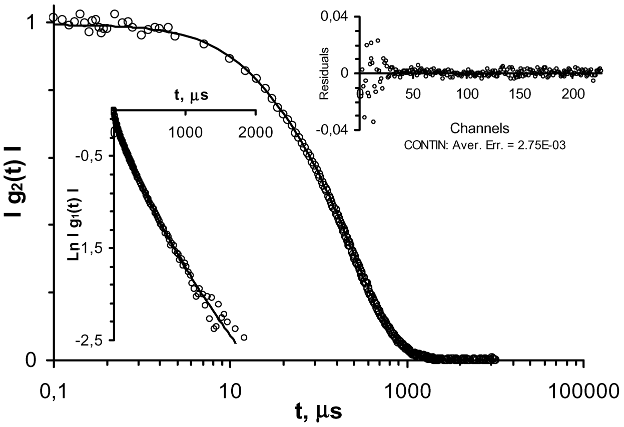

Fig. 3. Correlation function of scattered light intensity $g_2(t)$ obtained for sample 3 ($M_{PVP} = 10^4$ and 0.21 wt%) at 90° scattering angle and 1.4 mg/ml concentration. Insets show correlation function of electric field $g_1(t)$ and residuals. Solid line represents fit calculated by CONTIN and corresponds to the distribution of hydrodynamic radius presented in Fig. 8(b).

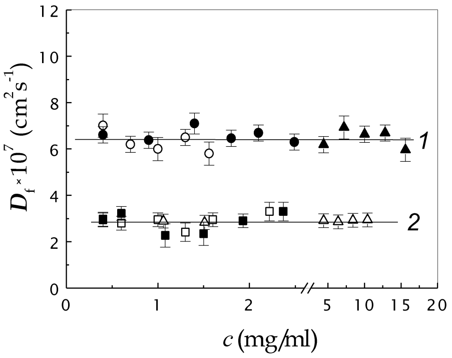

Fig. 4. Concentration dependence of the fast diffusion D_f for sample 1 (open circle) and sample 3 (solid circle) having $M_{PVP} = 10 \times 10^3$ (Curve 1) and for sample 6 (open square) and sample 7 (solid square) having $M_{PVP} = 40 \times 10^3$ (Curve 2). Diffusion coefficients of single PVP molecules of corresponding molar masses are plotted in the same scale vs. PVP–C_{70} concentration: $M_{PVP} = 10 \times 10^3$ (solid triangle) and $M_{PVP} = 40 \times 10^3$ (open triangle). Data obtained at scattering angle 90°.

Fig. 4 shows the concentration dependence of D_f in the aqueous solutions of PVP–C_{70} (samples 1, 3, 6, 7) at 90° scattering angle. Diffusion coefficients D_f remain constant with dilution. It was observed that the fast diffusion coefficient does not depend on q^2.

To understand the nature of the fast mode, investigations of aqueous PVP solutions with no added fullerene were performed. Correlation functions of aqueous PVP solutions were single exponential. In Fig. 4, translation diffusion coefficients of pure PVP samples are plotted as a function of concentration of the corresponding PVP–C_{70} (samples 1, 3, 6, 7), assuming that the concentrations of PVP–C_{70} and of pure PVP are the same. Translation diffusion coefficients of pure PVP are independent of the PVP concentration and coincide with the fast diffusion coefficients of the PVP–C_{70} solutions. One may conclude that the fast modes of the solutions represent single PVP molecules. However, the fast mode may also include PVP–C_{70} complexes consisting of a single PVP molecule bound to a single C_{70} molecule. So, using Stokes–Einstein equation the translation diffusion coefficient of C_{70} was estimated, assuming a hard sphere with a radius of 0.35 nm (for fullerene) [19]. The diffusion coefficient equals 0.6×10^{-7} cm^2/s and it is one order of magnitude lower than the diffusion coefficient of a single PVP molecule. Therefore, the fast diffusion describes the motion of a single PVP chain or that of a single chain into which one or few fullerenes are bound.

Relative intensities of the slow mode are higher than those of the fast mode for about 1–2 orders of magnitude. Deviation of the correlation function from a single exponential form may be attributed to the polydispersity of the sample. The polydispersity in this case is due to the presence of two types of scatterers in the solutions: individual molecules of PVP and large IMC PVP–C_{70}. Correspondingly, two different coefficients, D_f and D_s, were

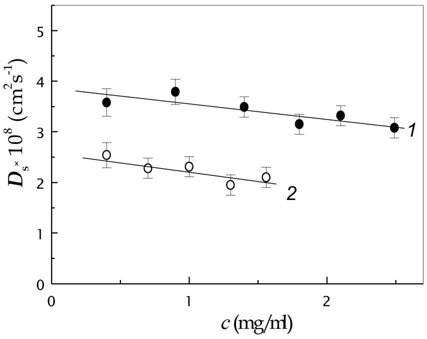

Fig. 5. Concentration dependence of the slow diffusion coefficient D_s for solutions of: sample 3 (1) and sample 1 (2). Data obtained at 90° scattering angle.

observed. Existence of two types of diffusion was also confirmed using an interferential diffusometer of Tsvetkov's type (where chemical potential is a driving force of the diffusion process) [16].

Fig. 5 shows the concentration dependencies of D_s observed for the sample 3 containing 0.21 wt% C_{70} (Line 1) and the sample 1 containing 0.63 wt% C_{70} (Line 2). These two samples originate from the same matrix PVP with a molar mass $M_{PVP} = 10^4$. As can be seen from the figure, the slow diffusion coefficients of both samples increase with decreasing the solution concentration. This may be associated with the disintegration of the complexes upon dilution: the complexes separate into smaller fragments of similar internal organization. This is not the case for the solutions of the samples based on higher molar mass PVP. Concentration dependencies of D_s for samples based on higher molecular weight PVPs (samples 6 and 7 with $M_{PVP} = 40 \times 10^3$ and sample 8 with $M_{PVP} = 46.3 \times 10^3$) are shown in Fig. 6. The slow diffusion coefficients of samples 6, 7, and 8 were found to be independent of concentration. This can be rationalized in terms of a competition between the hydrophobic attraction of C_{70} molecules and the volume effects of PVP molecules of the complex, i.e. C_{70} molecules form interchain links while slowly diffusing large PVP chains prolong the intermolecular contacts. It is also possible that polymers with a high chain length entangle and stabilize the complexes.

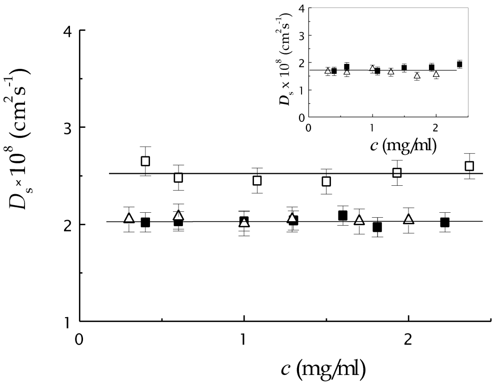

Fig. 6. Dependence of D_s on concentration for aqueous solutions of sample 7 with $M_{PVP} = 40 \times 10^3$: $C_{ful} = 0.40$ wt% (open square) and $C_{ful} = 0.63$ wt% (sample 6, solid square), with $M_{PVP} = 46.3 \times 10^3$ and $C_{ful} = 0.55 \times$ wt% (sample 8, triangle), recorded at 90° angle. Inset demonstrates the concentration dependence of D_s for sample 6 and 8 at 0° scattering angle.

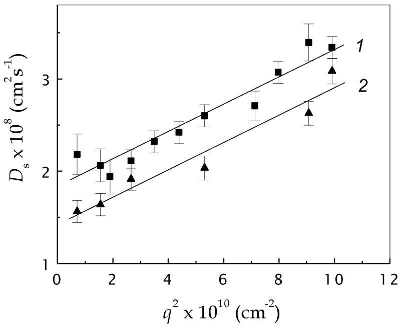

Fig. 7. Angular dependence of D_s for sample 7 at concentration 2.4 mg/ml (1) and sample 8 at concentration 2.0 mg/ml (2).

Slow diffusion coefficients correspond to particles large in comparison to the incident light wavelength. Therefore, the slow diffusion coefficients were measured for samples 7 and 8 at various angles and extrapolated to zero scattering angle. Inset in Fig. 6 shows the concentration dependence of the zero scattering angle D_s, similar to the one obtained at 90°.

Concerning the angular dependencies of the slow diffusion coefficients of samples 7 and 8, the D_s vs. q^2 appeared to be an increasing function of angle, as is evident from Fig. 7. q^2 dependence of D_s has a positive slope characteristic to a translational diffusive process. For this reason, D_s describes the translation of IMC PVP–C_{70}.

It ought to be stated here that the relative peak intensities of the size distributions do not significantly change upon dilution, see Fig. 8. The positions and the shapes of the peaks are constant. This finding correlates with the results presented in the inset of Fig. 2. Indeed, if the size and ratio of single PVP molecules and IMC PVP–C_{70} does not change with dilution, dissymmetry of scattered light

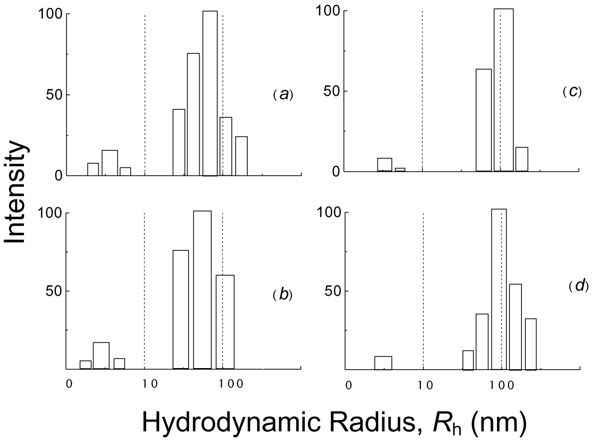

Fig. 8. Histograms of the size distribution obtained from DLS experiments on aqueous solutions of PVP–C_{70} complex ($M_{PVP} = 10^4$) with 0.21 wt% (a, b; sample 3) and 0.63 wt% (c, d; sample 1) of fullerene. Solution concentrations: 2.1 mg/ml (a), 1.4 mg/ml (b), 1.6 mg/ml (c), and 1.3 mg/ml (d). Data collected at 90° scattering angle.

intensity does not change. On the other hand, the peak corresponding to the slow diffusion coefficient shifts towards larger particle size upon increasing the fullerene content (C_{ful}) in the complex. The relative amplitude of the fast mode decreases because scattering from larger objects swamps the light scattered by single PVP molecules.

Two diffusive modes have previously been observed also for PVP–C_{60} complexes [9]. However, for PVP–C_{60} complexes in contrast to PVP–C_{70}, no diffusion coefficients corresponding to individual PVP chains were observed. The diffusive mode of the order of 10^{-8} cm^2/s existed in both PVP–C_{60} and PVP–C_{70} solutions. This mode was the fast mode for PVP–C_{60} and the slow one for PVP–C_{70}. The slow mode of PVP–C_{60} solutions was of the order 10^{-9} cm^2/s and has not been observed for PVP–C_{70} solutions. This mode was interpreted in terms of strong intermolecular interaction in solutions. Apparently, the intermolecular interaction in the PVP–C_{70} solutions is weaker than in PVP–C_{60} and cannot be detected by DLS.

5. Conclusions

It has been shown using light scattering that, PVP molecules form large intermolecular complexes with C_{70} in aqueous solutions. Hydrophobic fullerene binds to PVP and forms a water soluble complex. Apparently, a fullerene molecule is capable to bind two or more PVP molecules forming a multimolecular associate. An increasing number of fullerene molecules binds more PVP macromolecules into the complex. This is supported by the data in Table 1. Thus, the molecular weight and dimensions (R_g and $R_{h,s}$) of the intermolecular PVP–C_{70} complex increase with increasing fullerene content when M_{PVP} is kept constant. If the fullerene content is fixed, increase in the molecular weight of the matrix PVP causes an increase in the total molecular weight and the size of the complex.

Large dimensions of the complex do not allow a star/micellar-like conformation having a core of hydrophobically associated C_{70} molecules. It is expected that the PVP–C_{70} complex has a transient network structure. In the complex, fullerenes serve as junction points for two or more molecules of PVP. $R_g/R_{h,s}$ ratio for IMC PVP–C_{70} can be estimated for sample 8 using the data obtained at zero scattering angle when no single PVP molecules were detected. The ratio $R_g/R_{h,s}$ is 1.7, which is typical for swollen structures. IMC PVP–C_{70} is stable and does not disaggregate upon dilution when $M_{\mathrm{PVP}} > 40 \times 10^3$. For these samples no concentration dependence of D_s was observed. Dissymmetry of the scattered light intensity does not change with concentration showing that the ratio of single PVP molecules and intermolecular PVP–C_{70} complex is constant.

The solutions of PVP–C_{70} also contain a certain quantity of single PVP molecules not bound to fullerenes. The fullerene content in PVP–C_{70} samples investigated is rather small. It may explain the existence of free polymer molecules in samples based on shorter PVP chains. Low number of fullerene molecules cannot bind all short PVP molecules into the complex. The same weight fraction of fullerene molecules may bind even all PVP molecules with longer chain length because of the total number of longer PVP molecules is smaller for the same C_{70}/PVP weight ratio. Actually, there is a certain C_{70}/PVP molar ratio, which cannot be exceeded. Above this molar ratio, free fullerene molecules appear, which are not bind to PVP; PVP chains become saturated with fullerene and the fullerene molecules are no longer soluble in water. With lower fullerene concentration, free PVP molecules may exist in solutions.

The comparison of aqueous solutions of PVP–C_{60} and PVP–C_{70} unequivocally indicates the organization of associative structures in both systems. However, there are significant differences in properties of PVP–C_{60} and PVP–C_{70} complexes. First of all M_w for IMC of PVP–C_{70} is lower than those for PVP–C_{60} by a factor of 2.5–3. As a result, the critical concentration of PVP–C_{70} in solutions is higher than that of PVP–C_{60} (0.20 and 0.14 g/dl, respectively). DLS experiments revealed a considerable difference in diffusion coefficients and in hydrodynamic behavior of PVP–C_{60} and PVP–C_{70} complexes in general. Thus no individual PVP macromolecules were detected for PVP–C_{60}, while strong interaction between PVP–C_{60} complexes results in a long-range organization in solution. The latter was not observed for PVP–C_{70} solutions. Another difference is the depolarization and dissymmetry of scattered light, which have not been observed in PVP–C_{60} solutions. Because of all the experimental conditions (the way of preparation of complexes, the range of M_w of matrix polymer PVP, the fullerene content in the complexes) were identical both for PVP–C_{60} and PVP–C_{70}, one can suggest that the cause of differences mentioned above is an asymmetrical π-electron structure of C_{70}. Owing to this heterogeneity of electronic density, C_{70} forms smaller and less ordered (less interacting) nano-structures in aqueous solution.

Acknowledgements

Elvira Tarassova acknowledges the Laboratory of Polymer Chemistry, University of Helsinki for research grant provided. Authors also acknowledge Dr I.A. Baranovskaya for useful discussions, Dr S.V. Valueva for flow birefringence measurement, and especially the Institute of Experimental Medicine of the Russian Academy of Science and Dr L.B. Piotrovskii for preparation of the PVP–C_{70} samples.

References

[1] Friedman SH, Ganapathi PS, Rubin Y, Kenyon GL. J Med Chem 1998;41:2424.

[2] Da Ros T, Prato M. Chem Commun 1999;663.

[3] Ikeda A, Hatano Ts, Kawaguchu M, Suenaga H, Shinkai S. Chem Commun 1999;1403.

[4] Orfanopoulos M, Kambourakis S. Tetrahedron Lett 1995;36:435.

[5] Rio Ya, Nierengarten J-F. Tetrahedron Lett 2002;43:4321.

[6] Vinogradova LV, Melenevskaya EYu, Khachaturov AS, Kever EE, Litvinova LS, Novokreshehova AV, Sushko ML, Klenin SI, Zgonnik VN. Polym Sci 1998;40:1854.

[7] Khairullin II, Chen Yu-H, Hwang L-P. Chem Phys Lett 1997;275:1.

[8] Andrievsky GV, Kosevich MV, Vovk OM, Shelkovsky VS, Vashchenko LA. J Chem Soc Chem Commun 1995;1281.

[9] Sushko ML, Tenhu H, Klenin SI. Polymer 2002;43:2769.

[10] Klenin SI, Sushko ML, Dumpis MA, Poznyakova LI, Piotrovskii LB. J Techn Phys 2000;45:312.

[11] Sushko ML, Aseyev VO, Tenhu H, Klenin SI. Mol Mater 2000;13:339.

[12] Sushko ML, Klenin, Dumpis MA, Poznyakova LI, Piotrovskii LB. Techn Phys Lett 1999;25:778.

[13] Sushko ML, Baranovskaya IA, Bykova EN, Klenin SI. J Mol Liq 2001;91:59.

[14] Gribov LA, Novosadov BK. Russ J Struct Chem 1999;40:582.

[15] Yamakoshi YN, Yamagami T, Fukuhara K. J Chem Soc Chem Commun 1994;517.

16. (a) Tsvetkov VN. Rigid-chain polymers: hydrodynamic and optical properties in solution. New York: Consultants Bureau; 1989. (b) Kratochvil P. Classical light scattering from polymer solution. Amsterdam: Elsevier; 1987.

[17] Siegert AJF. MIT Rad Lab Rep No 4652; 1943.

[18] Anufrieva EV, Krakovyak MG, Nekrasova TN, Ananieva TD, Sheveleva TV, Piotrovskii LB. International IUPAC Symposium, Book of Abstracts:156. ; 2002.

[19] Eletskii AV, Smirnov BM. Uspehi fizicheskih nauk 1995;165:977.